Removal of Organic Films from Solid Surfaces Using Aqueous Solutions of Nonionic Surfactants. 1. Experiments

Stephen P. Beaudoin, Christine S. Grant, and Ruben G. Carbonell*

Department of Chemical Engineering, North Carolina State University, Box 7905, Raleigh, North Carolina 27695-7905

An important step in the production of printed wiring assemblies (PWAs) is the postsolder removal of flux residues from the surface. Traditionally, this has been accomplished using CFC-113-based solutions, but the Montreal Protocol and the Clean Air Acts have forced the development of alternative cleaners. This is a study of the mechanisms by which aqueous solutions of a nonionic surfactant (pentaethylene glycol mono-*n*-dodecyl ether ($C_{12}E_5$)) remove films of flux residues (abietic acid in isopropyl alcohol) from PWA surfaces. Cleaning rates were studied in a rotating disk apparatus to control hydrodynamic conditions. The cleaning process followed a three-step mechanism. In the first stage, surfactant liquefies the organic by partitioning into the film. In the second and third stages, shear stresses at the PWA surface remove aggregates of the surfactant-laden liquefied AA from the bulk AA film and the PWA substrate, respectively.

Introduction

An important step in many industrial manufacturing processes is the decontamination of solid surfaces. One such application, the cleaning of flux residues from printed wiring assemblies (PWAs), has traditionally been accomplished using CFC-113-based cleaning solutions. The use of these solutions is limited by the Montreal Protocol and the Clean Air Acts, and there is research underway to develop alternative PWA cleaners. The work presented here has two aims: to investigate the possibility of using aqueous nonionic surfactant solutions as CFC-113 replacements for PWA cleaning and to understand the mechanisms involved when aqueous surfactant solutions are used to clean flux residues from PWAs.

Printed Wiring Assembly Contaminants and Cleaners. In the assembly of PWAs, flux is used to clean the metallic leads of circuit boards and electronic components that are to be soldered together. Flux has many formulations, depending on the type of PWA being processed, the type of soldering process being utilized, and the type of flux residue remover being applied. Traditional rosin-based flux formulations are composed of 10−40% organic solids, and abietic acid (AA) is the primary component of these solids. The balance of the flux is composed of carriers, such as isopropyl alcohol (IPA), and activators, such as diethylammonium chloride. The carriers comprise from 60 to 90% of the flux.

The activators in flux remove oxide layers and contaminants from the electrical leads on both the PWA and the components, and the AA coats the leads to prevent their recontamination prior to soldering (Woodgate, 1983). When molten solder contacts fluxed leads, it displaces the majority of the flux, leaving only small quantities of residue on the surface. These residues can interfere with the processing and performance of the PWAs, and many industrial and military specifications do not allow any flux residue to remain on circuit boards (Riza and Kesavan, 1989). For example, ionic (or polar) species within the residues can cause current leakage through the surface of the PWA and corrosion of metal surfaces on the board (Denison, 1975; Langan, 1989; Manko, 1986). While AA residues themselves do not hamper the performance of the PWA (Manko, 1986), they do interfere with standard "bed-of-nails" testing used to check the quality of electrical connections on the board. In addition, when AA resolidifies after the high temperatures found in soldering (up to 425 °C), it forms a shell-like matrix trapping the ionic components of the flux residue on the board. The structure of AA is presented below.

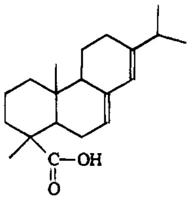

Abietic Acid

In typical industrial manufacturing processes for PWAs, vapor degreasing units use CFC-113- or HCFC-based cleaners to remove flux residues from surfaces (Andersen, 1989). Usually, the cleaners are azeotropic solutions with boiling points between 30 and 51 °C. Besides low boiling points, the cleaners share common traits of low viscosity and low contact angle on PWA substrates, so that they can penetrate into very narrow openings between the components and the substrate. Effective alternatives to CFC-113 also should spread rapidly over the PWA surface, penetrate into narrow openings, and rapidly solubilize the contamination, leaving behind no residues.

Surfactant-Based Cleaning Research. There is significant literature on the surfactant-based removal of oily soils from surfaces. This research has focused on understanding the mechanisms by which different surfactants solubilize different types of contaminants, with less effort spent in quantifying the rate-controlling steps involved in actual cleaning applications. The effect of hydrodynamics on surface cleaning is not well-understood.

Three important mechanisms have been identified in surfactant-based cleaning: roll-up, emulsification, and solubilization. In roll-up, surfactant preferentially wets

---

* Author to whom correspondence should be addressed. E-mail: ruben@ncsu.edu. Fax: (919) 515-3465.

0888-5885/95/2634-3307$09.00/0

the substrate, reducing the contact angle at the oil–substrate–water contact line. This causes the area of oil–substrate contact to shrink and the oil to protrude into solution. The oil is then snapped-off from the interface by mechanical or hydrodynamic forces, leaving behind either a small amount of residue or a clean surface. Many authors have witnessed or inferred this behavior in surfactant systems (Aronson et al., 1983; Dillan, 1979; Dillan et al., 1979; Fort et al., 1968).

Mixing of surfactant and water into the oil (contaminant) phase or the mixing of oil and surfactant into a water-rich phase can lead to the formation of water-in-oil or oil-in-water microemulsions, respectively. These microemulsion phases may be displaced from the surface by hydrodynamic or mechanical action. Emulsification during cleaning has been observed directly by many authors (Cox et al., 1987; Mori et al., 1989; Neogi et al., 1985; Raney et al., 1987; Raney and Miller, 1987; Schambil and Schwuger, 1987).

Finally, solubilization is the incorporation of oil into micelles, surfactant liquid crystals, or other surfactant structures in the aqueous surfactant solution. The difference between emulsification and solubilization is that in solubilization, the solubilized material is in the same phase as the surfactant, while in emulsification, the solubilized material is present as a dispersion (Rosen, 1989). The partitioning of slightly water-soluble oil molecules into micelles is an example of solubilization. Many authors have witnessed solubilization-based cleaning or interpreted cleaning data based on solubilization considerations (Carroll, 1981; Carroll, et al. 1982; Nakagawa and Nakagawa, 1960; Sayeed and Schott, 1986; Schott and Sayeed, 1986; Shaeiwitz et al., 1981; Tokiwa, 1968).

The type of cleaning most pertinent to this work is emulsification-based cleaning. A review of the literature on this subject has been performed by Miller and Raney (1993). When nonionic surfactants are used to remove oily soils from hard and soft surfaces, partitioning of surfactant into the soil often occurs (Cox et al., 1987; Cox, 1990; Dillan et al., 1979). Temperature and surfactant activity in bulk solution were found to affect the surfactant partitioning. Dillan et al. (1979) and Schambil and Schwuger (1987) related increased surfactant partitioning rates into oily soil to increased temperature. Mankowich (1961) correlated soil removal with increased surfactant activity in solution. Finally, surfactant adsorption at oil–water and air–water interfaces, the precursor to surfactant partitioning, was found to be controlled in some instances by external mass transfer processes (Van Hunsel et al., 1986).

Another important parameter in surfactant-based cleaning is the oil–water interfacial tension, which is controlled by the polarity of the oily soil, the nature of the surfactant–soil interaction, and the system temperature. Dillan et al. (1979) reported that the water–oil interfacial tension determined the mechanism of release of oil beads into aqueous solution from solid surfaces. At the phase inversion temperature (PIT), a water-continuous phase containing surfactant and oil inverts to become an oil-continuous phase containing water and surfactant. An ultralow interfacial tension (less than 1 dyn/cm) exists between the oil and surfactant phases under these conditions. Many authors have found that optimal oil removal from surfaces occurs in the vicinity of the PIT of the surfactant–oil–water systems they studied (Mori et al., 1989; Raney and Benson, 1990; Raney et al., 1987; Schambil and Schwuger, 1987)

The type of surfactant phase present in solution affects the rate and extent of oil removal from solids. Raney and Miller (1987) found that optimal oil removal occurred when aqueous solutions contained dispersions of lamellar liquid crystalline surfactant and that an oil-in-water microemulsion formed during the cleaning. Mori et al. (1989), Raney et al. (1987), and Raney and Benson (1990) also noted rapid mixing of oil and aqueous phases and optimal cleaning, in the presence of either lamellar liquid crystal or L3 (sponge-like lamellar) phases. In a related study, Chiu et al. (1988) found that the rate of solubilization of oil into surfactant solutions was much greater when large surfactant aggregates were present than when monomeric surfactant was present. Finally, Neogi et al. (1985) noted that a four-phase system of oil–intermediate phase–lamellar liquid crystalline phase–micellar phase existed during the contacting of $C_{12}E_4$ (a nonionic surfactant) with decane.

There is evidence in the literature that it is more difficult to remove oil residues from solid surfaces at low surface coverages. Both Harris et al. (1961) and Mankowich (1961) noted a significant drop in the rate of removal of oily soils from hard surfaces after 90% removal. This suggests that soils bound at the substrate–soil interface are removed by a different mechanism than soils far from the interface.

Research addressing cleaning rates under controlled hydrodynamic conditions is limited. In studies of the removal of oily soils from contaminated disks using a rotating disk apparatus, Shaeiwitz et al. (1981) and Chan, et al. (1976) concluded that the initial rate of removal into a micellar nonionic surfactant solution was controlled by the desorption of oily aggregates from the disk surface. Carroll (1981) and Carroll et al. (1982) obtained a different result for the removal of liquid oil drops from polymer fibers into stationary micellar nonionic surfactant solutions. They postulated that the rate-limiting step in the oil removal was the adsorption and dissociation of surfactant micelles at the oil–water interface. The solubilization was observed microscopically, and no emulsification or other transformation of the oil phase during solubilization was apparent, so that micellar solubilization was indeed the cleaning mechanism. In the work of Shaeiwitz et al. (1981), the oil–water interface was not observed during the solubilization process; hence, the mechanism of micellar solubilization was inferred.

In summary, when nonionic surfactants are used to remove oily soils from surfaces, the surfactant first penetrates the soil, reducing the oil–water interfacial tension and the soil viscosity. Depending on the surfactant phase present and the ability of that phase to solubilize oil, the oil may be removed by either roll-up, solubilization, or emulsification. In the current research, the mechanisms by which micellar and submicellar solutions of a pure nonionic surfactant, penta ethylene glycol mono-*n*-dodecyl ether ($C_{12}E_5$, $CH_3(CH_2)_{11}O(CH_2CH_2O)_5H$), remove mixed films of abietic acid (AA) and isopropyl alcohol (IPA) from solid surfaces are evaluated under controlled hydrodynamic conditions using a rotating disk apparatus. In the first part of this study, disks were coated with a representative flux residue containing AA mixed with IPA, and the resulting coating was characterized. Next, the partitioning of the nonionic surfactant from aqueous solution into

Chart 1

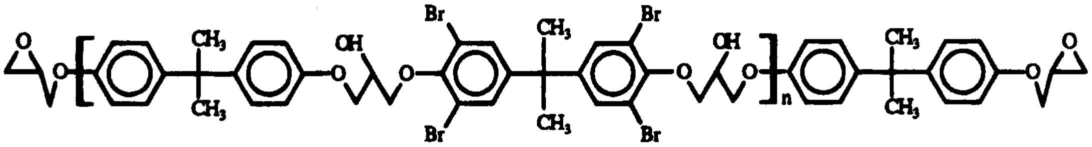

these AA/IPA coatings was quantified, and a study of the phases formed when aqueous $C_{12}E_5$ solutions contacted the AA/IPA films was conducted. Finally, the removal of the representative flux residues from PWA substrates was monitored continuously under controlled external mass transfer conditions in a rotating disk apparatus. These experiments allowed a detailed evaluation of the cleaning mechanism.

Experimental Procedures

Materials. The AA used in this study was supplied by Alfa Specialty Chemicals and was approximately 90% pure. The IPA and tetrahydrofuran (THF) were HPLC grade, from Fisher Scientific, and the $C_{12}E_5$ supplied by Nikko Chemicals of Japan was reported to be 99% pure. The water used in this work was 18.3 MΩ·cm DI water from a Barnstead Nanopure system. FR-4 laminate was used as the substrate in the cleaning experiments. It is a common PWA substrate, and it consists of layers of glass fabric epoxied together using brominated epoxy resins with chemical structures as shown in Chart 1 (Wang, 1988). The FR-4 laminate was donated by Northern Telecom in Research Triangle Park, NC.

The hydrophile–lipophile balance (HLB) of a surfactant is a commonly-used measure of its tendency to dissolve in aqueous solution or partition to an interface. Various authors have related surfactant HLB to cloud point and oil solubilization phenomena (Cox, 1990; Cox et al., 1987; Schott, 1969). The HLB of $C_{12}E_5$ is 11.67, as calculated from the formula (Rosen, 1989),

$$\mathrm{HLB} = 20\frac{M_H}{M_H + M_L} \qquad (1)$$

In this expression, M_H is the formula weight of the hydrophilic portion of the molecule [g] and M_L is the formula weight of the hydrophobic portion of the molecule [g]. For $C_{12}E_5$, M_H is 237, while M_L is 169. The critical micelle concentration (cmc) of $C_{12}E_5$ is 6.4×10^{-5} M.

Disk Coating and Characterization. Circular disks of FR-4 laminate with 1.1 cm radius were cut from flat sheets of FR-4. These disks were used in the rotating disk apparatus in the cleaning study described below. Flux residues on the surface of PWAs were simulated by spin coating mixed films of AA and IPA onto these disks. The coating solutions contained 42 ± 1% (by mass) AA dissolved in IPA.

In the spin coating process, 100 μL of the AA in IPA solution were placed on the center of a stationary disk on a Headway Research Inc. Model CB15 spin coating apparatus in a microelectronics clean room. After the solution was applied, the disk was accelerated rapidly to 2000 rpm and allowed to spin for 40 s. When the coating was completed, the disks were stored in a vacuum desiccator at room temperature for 24 h and then in a refrigerator until they were used in the cleaning experiments. If thicker coatings were desired, additional coatings were applied, after storage in the desiccator. Disks with one, two, and three coats were used. The disks were weighed twice, once before the coating process and then again just before the cleaning studies, to determine the mass of the coatings. A Denver Instruments AB-160 Analytical Balance was used to weigh the disks. The thicknesses of the films on the disks were estimated based on the amount of AA and IPA present on the disks (explained below). The mean thickness of each coating layer was approximately 10 μm. SEM analysis of the coated disks indicated that the AA/IPA films had smooth, nonporous, crack-free surfaces with some small-amplitude surface waves.

Two techniques were applied to determine the amount of IPA in the AA films after the coating and drying processes. First, the coated disks were immersed in 50 to 100 mL of THF for 30 s to dissolve the AA/IPA films. The AA content of the resulting solutions was determined on a Schimadzu 2101 spectrophotometer set at 241 nm, by comparison with the absorbance of standard solutions of known AA concentration. The mass of AA recovered in the THF was compared to the mass of the coating to determine the fraction of the film which was composed of AA. The second method utilized disks which had been used in the cleaning experiments. After each cleaning run, the amount of AA which had been removed from the disk by the surfactant solution was known. Each disk was then agitated vigorously for 30–60 min in an aqueous solution containing 1×10^{-2} M $C_{12}E_5$. Any AA which remained on the disk after the cleaning experiment was extracted into this solution, and its absorbance was measured on the Schimadzu 2101 spectrophotometer at 241 nm. The amounts of AA recovered during the cleaning and extraction steps were compared to the mass of the film initially present on the disk to determine the fraction of AA in the film. The mean results between the experiments using extraction in THF and the cleaning/$C_{12}E_5$ extraction technique agreed to within 5%.

Partitioning of $C_{12}E_5$ into the AA/IPA Films. Disks of FR-4 with a single coating of AA/IPA were suspended in 500 mL of aqueous solutions of varying $C_{12}E_5$ concentration for times ranging from 2 to 12 days. After contacting, the disks were removed from the solutions and agitated in 50 mL of THF for 30 s to extract the AA and $C_{12}E_5$. The resulting solutions were passed through a gel permeation chromatography (GPC) separation train with a mobile phase of THF flowing at 1 mL/min using a Waters 6000A isocratic pump. Two Shodex kf-801 gel permeation columns in series were used. The injections were performed with a Rheodyne injector with a 200 μl liquid-phase injection loop. A Waters 440 UV absorbance detector set at 254 nm (AA has a broad absorption band that includes 254 and 241 nm) and a Waters 410 differential refractometer (RI apparatus) were placed immediately downstream of the columns. The UV detector was calibrated for the AA, while the RI apparatus was calibrated for the $C_{12}E_5$. The chromatography and cleaning (discussed below) results were analyzed using a Waters Maxima Chromatography Software system.

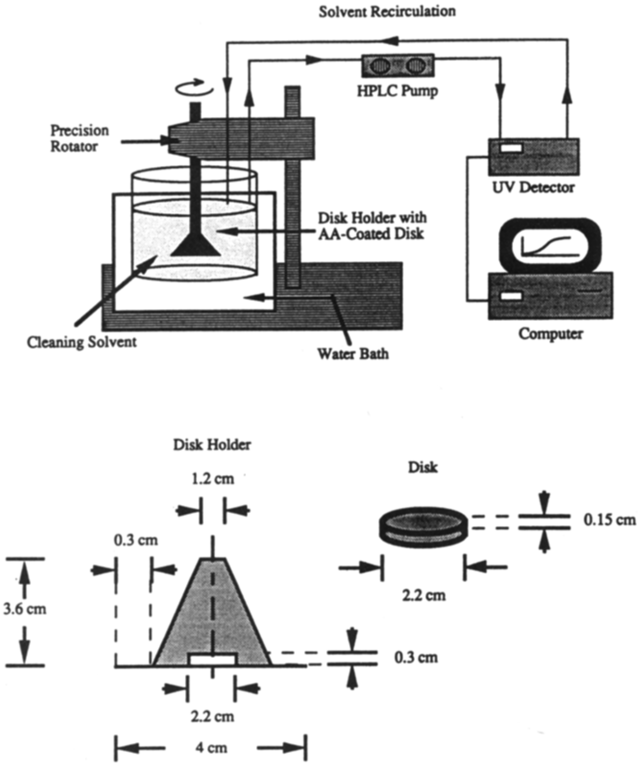

Figure 1. Rotating disk cleaning apparatus and disk holder.

Contacting Experiments To Determine Dynamic Phase Behavior. It is important to understand the phase behavior resulting from the contact of the surfactant solutions with the AA/IPA films. This was accomplished by scraping the AA/IPA films off several uncleaned disks with a razor blade, placing the scrapings in a glass capillary with surfactant solution, and viewing their behavior under an optical microscope. The capillaries were manufactured by VitroDynamics (0.8 mm path length, 8 mm width, rectangular capillaries). They were flame-sealed at one end prior to the start of each experiment. After locating the particles through polarized light on an optical microscope (Olympus BH-P), aqueous solutions of $C_{12}E_5$ were added and the contacting behavior was observed. The microscope was equipped with an Olympus C-35 AD2 camera and photographic system which allowed pictures to be taken during contacting. A red filter was employed to assist in the detection of birefringence exhibited by liquid crystalline phases. The capillaries were maintained at the temperature used in the cleaning experiments (24 °C) through the use of a hot stage (Sensortek TS-4 ER Controller and hot stage).

Cleaning Experiments. The cleaning experiments were conducted using a rotating disk apparatus, as shown in Figure 1. The disks were carefully machined so that they could be press-fit into a tapered Teflon holder. No gap existed at the edge of the disk where it contacted the holder. The holder/disk assembly was attached to the shaft of a Pine Instruments AFMSRX analytical rotator and immersed in a 600 mL beaker containing 500 mL of aqueous $C_{12}E_5$ solutions of known concentration. The solutions were made by pipetting a known volume of surfactant into the beaker containing DI water and stirring for approximately 15 min to disperse the surfactant. The surfactant concentrations ranged from 6×10^{-5} to 4.1×10^{-3} M. During the experiments, the beaker of cleaning solution was held in a water bath at 24 °C. Immediately after immersion into the cleaning solution, the shaft was rotated at a constant speed, ranging from 350 to 2000 rpm. The Reynolds number (*Re*), based on the disk radius and linear velocity at the outer edge of the disk, was always less than 2×10^5, the critical number for transition from laminar to turbulent flow in a rotating disk apparatus (Mohr and Newman, 1976). The cleaning solutions were circulated continuously through a Waters 440 UV absorbance detector set at 254 nm and returned to the beaker using a Waters 6000A HPLC pump at a flow rate of 10 mL/min. The residence time of the solution in the analytical loop was approximately 1 min. The cleaning experiments lasted from 2 to 15 h. The absorbance reading on the UV detector was recorded electronically once every second. After the disks were cleaned, they were extracted in a solution of 1×10^{-2} M $C_{12}E_5$ as discussed above. The disks were weighed before and after the coating process and again after the extraction process, so that the mass of the coating, the IPA fraction of the coating, and the extent of the cleaning could be determined.

As the disk rotates, fluid from the bulk solution is drawn to the disk surface and slung off the outer edges of the disk. The elements of the three-dimensional flow field and the mass transfer coefficient for transport of solutes to and from the surface of the rotating disk have been determined analytically and verified experimentally (Albery and Hitchman, 1971; Cochran, 1934; Daguenet, 1968; Ellison and Cornet, 1971; Levich, 1942; Mohr and Newman, 1976; Newman, 1966, 1973; Schlicting, 1968; White et al., 1976). Under laminar flow conditions, the mass transfer coefficient is given by

$$k_m = 0.6205\nu^{-1/6}D^{2/3}\omega^{1/2} \qquad (2)$$

where k_m = mass transfer coefficient in fluid phase [cm/s], ν = kinematic viscosity [cm^2/s], D = diffusion coefficient for solute in solution [cm^2/s], and ω = rotational speed of disk [rad/s]. The shear stress at the disk surface is given by (Middleman, 1987; Strong and Middleman, 1989),

$$\tau_{rz} = 0.51\nu^{-1/2}\mu r\omega^{3/2} \qquad (3)$$

where τ_{rz} = shear stress in the radial direction on the disk surface [g/cm·s^2], r = radial position on disk surface [cm], and μ = viscosity of fluid [g/cm·s].

It is important to note that the mass transfer coefficient for transport of solutes to and from the disk surface is proportional to $\omega^{1/2}$, while the shear stress is proportional to $\omega^{3/2}$. The reduction of $[Fe(CN)_6]^{3-}$ at a Ni electrode was used to verify that the rotating disk apparatus used in the cleaning experiments satisfied eq 1 (Cobo et al., 1972). The measured mass transfer coefficients agreed with theoretical predictions to within 4%, with reproducibility within 4%.

Results and Discussion

Characterization of AA/IPA Films. The results of the extraction studies using both THF and $C_{12}E_5$ are presented in Figure 2. For disks with one coating, approximately 25% of the coating is IPA. The disks with two and three AA/IPA coats contain approximately 35% and 45% IPA, respectively. It is apparent that for films with multiple coatings, IPA diffuses into the underlying layers, resulting in higher overall IPA concentrations. As the films harden, the outer surface dries first,

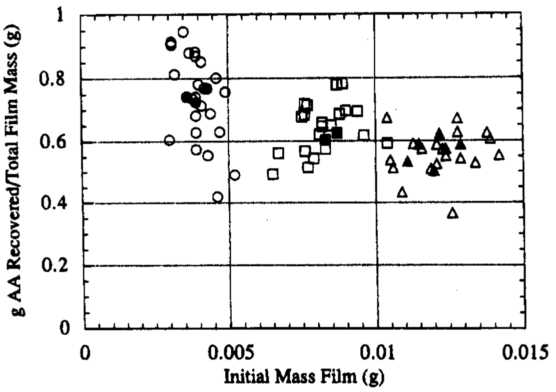

Figure 2. Mass fraction AA in films (●, ○, disks with 1 AA/IPA coat; ■, □, disks with 2 AA/IPA coats; ▲, △, disks with 3 AA/IPA coats; hollow symbols, clean and $C_{12}E_5$ extract; filled symbols, THF extract only.

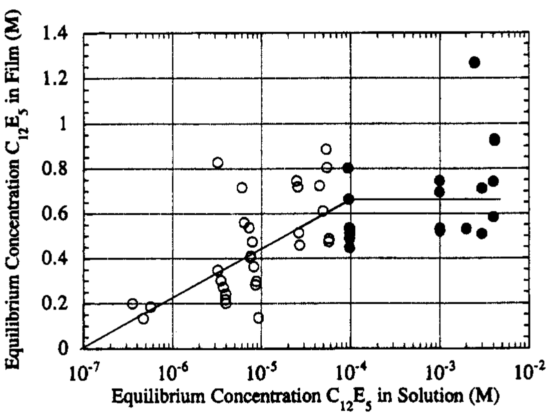

Figure 3. Partitioning of $C_{12}E_5$ into AA/IPA films: 24 °C, disks with 1 AA/IPA coat (○, below cmc; ●, above cmc).

forming a nonporous shell which traps the additional IPA in its core.

There are several sources of the scatter in Figure 2. Oxidation of the AA occurred during the disk-cleaning processes, as well as during the preparation of the coating solutions. This caused the UV absorbance of the AA removed from the disks to vary in a small but uncontrollable manner. Also, the extraction of residual AA from the surface of disks that had been used in cleaning studies involved the dissolution of extremely small quantities of AA into comparatively large volumes of aqueous surfactant solutions. This resulted in solutions whose UV absorbance approached the lower limit of detection, introducing error into the calculated AA concentrations. In contrast, disks that were extracted directly into THF without being used in cleaning experiments provided much more reproducible values of the mass fraction of AA in the films. The values obtained by this method are in the center of the ranges produced by the cleaning and extraction steps. While every attempt was made to minimize the error due to oxidation and the cleaning/extraction process, it was difficult to eliminate altogether.

Partitioning of $C_{12}E_5$ into AA/IPA Films. Figure 3 presents the results of the partitioning experiments. At surfactant concentrations below the cmc (6.4×10^{-5} M), the concentration of surfactant in the film in equilibrium with the bulk solution increased with increasing bulk concentration. However, this effect was linear on a semilog scale, and nonlinear in natural coordinates, suggesting a nonideal phase behavior. The surfactant concentrations in the film were high (0.1–0.7 M) compared with the solution concentrations (1×10^{-6}–1×10^{-3} M), indicating a large degree of partitioning into the AA. Above the cmc, the partitioning was essentially independent of the surfactant concentration. This is consistent with the fact that the surfactant activity is constant above the cmc. It is commonly observed in surfactant systems that the interfacial tension of surfactant solutions decreases with increasing surfactant concentration below the cmc but is independent of surfactant concentration above the cmc (Rosen, 1989). This phenomenon is consistent with the results of the partitioning experiments.

During the partitioning experiments, it was noted that when concentrated surfactant solutions (well above the cmc) were used, a bluish layer formed adjacent to the disk surface. Slight agitation dispersed this phase into small aggregates, which retained their identity in solution for short times before dissolving. This layer may have been a new phase formed by the swelling of the AA layer as surfactant and water penetrated, or it may have been caused by aggregation of surfactant near the film–solution interface. It is unclear at this time whether or not this layer had the same structure and composition as the films present on the FR-4 laminate. The fact that the pieces of this bluish layer which were shaken from the interface subsequently dissolved in solution suggests that the layer contained large amounts of surfactant and water. The formation of oil-in-water microemulsions at oil–water interfaces has been observed in other systems (Chiu et al., 1988; Mori et al., 1989; Raney and Miller, 1987).

The scatter in the data shown Figure 3 is attributed to several effects. The residual quantities of AA and $C_{12}E_5$ removed from the disk during the analysis of the partitioning were occasionally very low. As a result, the concentrations of these species in the THF were near the detection limits of the UV and RI detectors used. Also, the analytical technique (gel permeation chromatography) used for determining the concentration of AA and $C_{12}E_5$ in the THF solutions was difficult to operate in a highly reproducible manner. Small quantities of water in the sample caused variations in the peak areas and the quality of separation of the AA and $C_{12}E_5$, as did the byproducts of oxidation of the THF mobile phase. Finally, variations in the contacting time for the partitioning experiments may have allowed for varying degrees of oxidation of the $C_{12}E_5$. As with the data presented in Figure 2, these sources of error could not be eliminated entirely.

Phase Changes during Surfactant Adsorption. 1.0×10^{-2}, 4.1×10^{-3}, 1.0×10^{-3}, and 6.0×10^{-5} M solutions of $C_{12}E_5$ in water were contacted with the AA/IPA scrapings from coated disks. Sequential photographs were taken in time at 100× magnification at 24 °C to document the system behavior, and sample results are shown in Figure 4. These photos were taken in white light, and on the scale shown, one unit step is equal to 15 μm. At contact, the jagged nature of the outer edges of the crystals is apparent. As the surfactant penetrates into the AA, the jagged edges gradually disappear, and the crystalline regions of solid AA/IPA shrink. Finally, the AA becomes a liquid with a nearly spherical shape, with no crystalline regions visible. It is likely that this liquefied AA/IPA contains high concentrations of surfactant and water. Other photos of the same system were taken through polarized lenses, to detect the formation of liquid crystalline aggregates within the liquefied AA by the presence of bright birefringent regions in the liquefied AA crystals. No

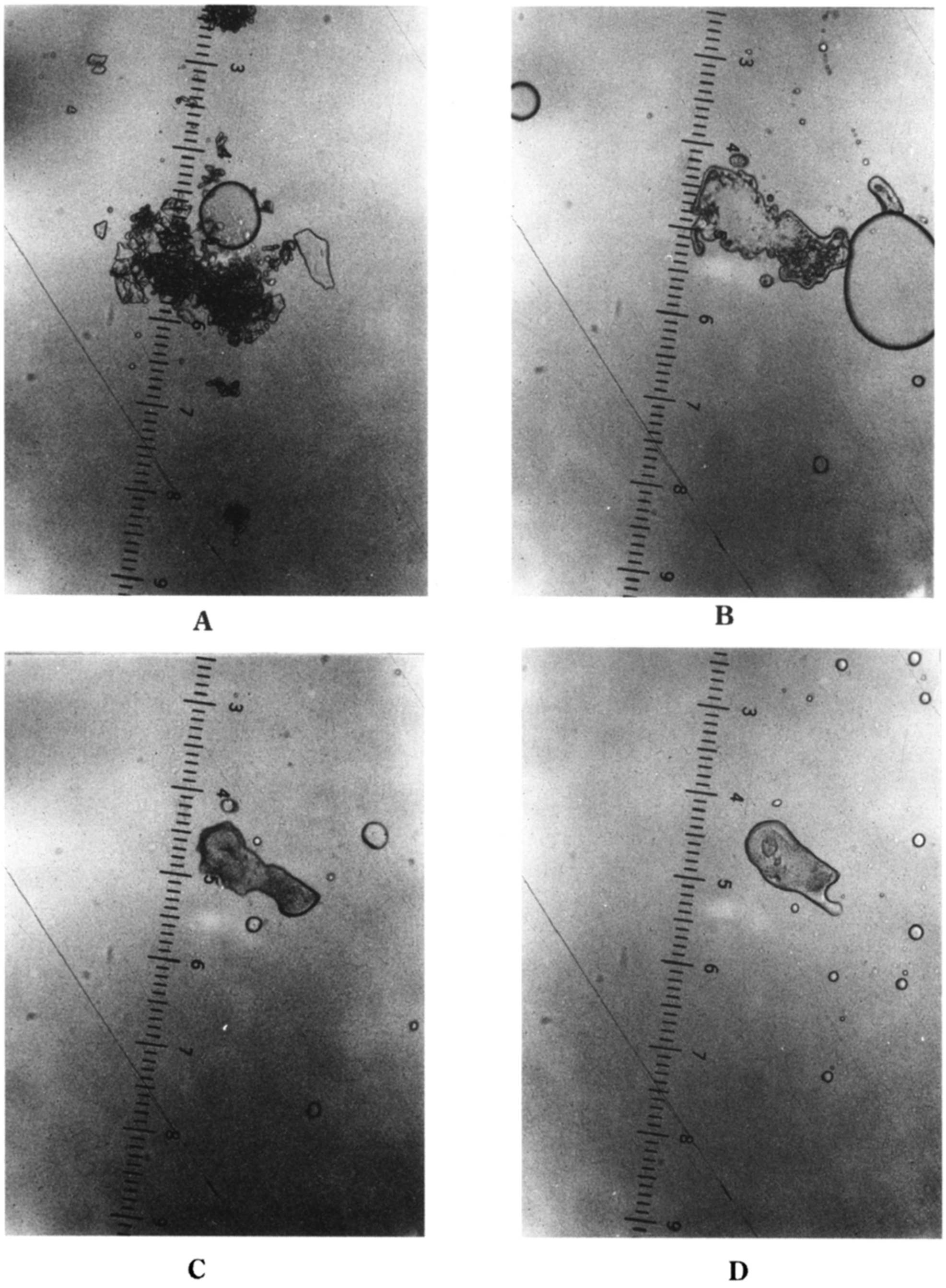

Figure 4. Contacting result, 4.1×10^{-3} M $C_{12}E_5$ with AA/IPA crystal, 24 °C, 100× magnification, 15 μm for 1 unit step on scale (reproduced at 65% of original size), white light; (A) at contact, (B) 33 min, (C) 55 min, (D) 79 min.

such regions were observed. The entire microscope was tilted during the liquefaction to check for flow birefringence (a characteristic of the sponge-like liquid crystalline L3 phase), but this effect was also not observed. It must be concluded that an isotropic phase of liquefied AA containing solubilized surfactant and water resulted from the surfactant penetration.

There was no tendency of the AA crystals to break up and be solubilized at any time during the liquefaction process, although in some cases small amounts of liquefied material were observed in the form of "halos" of AA droplets in the bulk solution surrounding the main AA/IPA crystals. As time progressed during contacting, the crystals lost their original shape and became more spherical. Often, they passed through a stage where a nonliquefied crystal remained inside a sphere of liquefied AA. Also, when two partially or completely liquefied crystals came into contact, they merged to form a large sphere of liquefied AA.

Observed Stages of Cleaning. Disks with 1 and 3 coats of the AA/IPA solution were used in the cleaning study. The rotational speed of the disks ranged from 350 to 2000 rpm, and the $C_{12}E_5$ concentration in solution varied from 6×10^{-5} M (submicellar) to 4.1×10^{-3} M (micellar). Since the apparatus records the absorbance of the cleaning solution once every second, the cleaning data resemble continuous lines when presented over long time intervals. The larger points on the lines in Figures 5–8 are present only to differentiate the different data sets.

Results of a typical cleaning experiment, presented in Figure 5 for an experiment at 1750 rpm with one AA/IPA coat on the disk and 4.1×10^{-3} M $C_{12}E_5$, indicate that the cleaning proceeds in three distinct stages. In

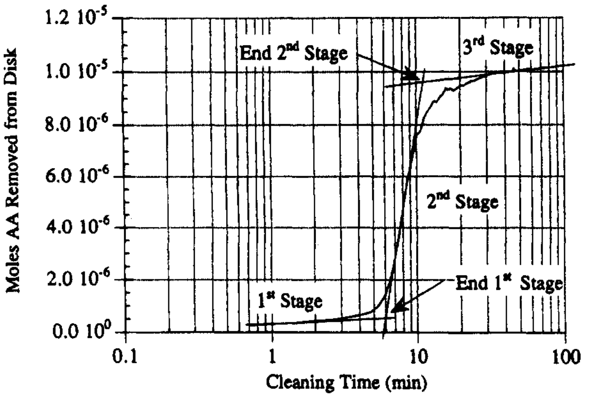

Figure 5. Typical cleaning result: 4.1 × 10^{-3} M $C_{12}E_5$, 1750 rpm, disk with 3 AA/IPA coats, 24 °C.

the first stage, small amounts of AA are removed from the surface. It is hypothesized that during this stage, solubilization-based cleaning occurs at the film–solution interface while surfactant penetrates into the bulk AA/IPA film and liquefies it. This penetration step is supported by the partitioning results presented above and the results of other studies in the literature with similar systems (Aronson et al., 1983; Cox, 1990; Cox et al., 1987; Dillan et al., 1979; Mankowich, 1961; McGuire and Matson, 1975; Schambil and Schwuger, 1987). It is also likely that the first stage ends when enough surfactant has penetrated into the film to lower its viscosity and/or interfacial tension to the point where external hydrodynamic or mechanical forces can pull elements of the film from the surface. The threshold level of surfactant required in the film to induce the change from the first to the second stage is affected by parameters which affect the hydrodynamic and mechanical forces acting on the disk surface, such as the disk rotational speed. For analytical purposes, the end of the first stage was established by drawing lines through the linear portions of the first and second cleaning stages of each data set and taking the intersection of these lines as the time for the end of the first stage. This method is illustrated in Figure 5. As a check, a straight line was fit (least squares) to the first stage cleaning data, and the end of the first stage was taken as the time at which the experimental data rose above the line by 5%. The agreement between these two methods was excellent.

During the second stage, films which have been completely or partially liquefied during the first stage are removed from the disk surface by hydrodynamic (shear) forces. The results of the contacting experiments indicate that surfactant penetration into the AA/IPA films greatly reduces the film viscosity. This facilitates the removal of aggregates of liquefied film during the second stage. As the aggregates are pulled from the disk, a new film–solution interface is created. The ability of surfactant in solution to reduce the free energy of interaction across the new interface also affects the cleaning during the second stage. For analytical purposes, the end of the second stage was determined by drawing asymptotic lines to the linear portions of the second and third cleaning stages of each data set. The intersection of these lines was taken to be the end of the second stage and the start of the third stage, as illustrated in Figure 5.

During the third stage, the AA removal approaches 100% asymptotically. Several experiments were conducted in which the third stage was allowed to continue until apparently no additional AA was being removed from the disk. On the basis of the original mass of AA on the disk and the concentration of AA in solution at the end of these experiments, it was determined that the third stage resulted in nearly 100% removal. Due to the slow rate of cleaning during the third stage, most of the experiments were stopped prior to 100% AA removal but after the shape of the third stage was established. For this reason, the duration of the third stage is not discussed below. Several cleaning experiments were stopped during the third stage, and the substrate was observed. The presence of "islands" of AA surrounded by bare FR-4 space was apparent on the surface of the disks during this stage. To remove these islands, the AA/IPA–water–FR-4 contact line must be separated from the interface by shear stresses. As can be seen in Figure 5, this is apparently a much slower, and quite different, process than the aggregate removal in the second stage. In fact, the third stage cleaning may resemble cleaning by the "roll-up" mechanism discussed previously. Harris et al. (1961) and Mankowich (1961), also found that the removal of the last elements of oily soil from surfaces was slower than removal of earlier elements.

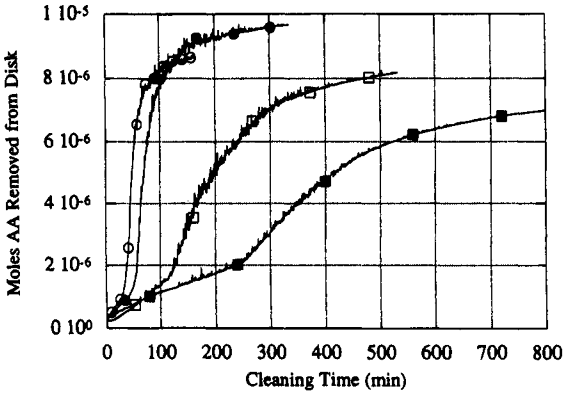

Figure 6. Effect of disk rotational speed on cleaning: 6 × 10^{-5} M $C_{12}E_5$, disk with 1 AA/IPA coat, 24 °C (○, 2000 rpm; ●, 1250 rpm; □, 700 rpm; ■, 525 rpm).

Effect of Disk Rotational Speed on Cleaning. The effect of the disk rotational speed on the three cleaning stages is illustrated in Figure 6 with experiments using 6 × 10^{-5} M $C_{12}E_5$ and disks with one AA/IPA coating. The duration of the first stage decreases with increasing disk rotational speed, and in general, the number of moles of AA removed from the disk in the first stage increases with decreasing disk rotational speed (longer duration of the stage). Compared to the second and third stages, the number of moles of AA removed during the first stage is very small. As mentioned above, it is believed that penetration of surfactant into the films occurs during the first stage, and this process is considered more important with respect to the overall cleaning process than the AA removal seen during the first stage. As the surfactant penetrates, the viscosity of the films decreases, and the first stage ends when the film viscosity has been reduced to the point that aggregates can be sheared from the disk surface. As discussed previously, the mass transfer coefficient for transport of surfactant to the disk surface is proportional to $\omega^{1/2}$, so that increasing the disk rotational speed increases the mass transfer rate significantly. Figure 6 suggests that when the external mass transfer rate is increased (higher rotational speed), the penetration rate also is increased (decreased duration of the first stage). Another way the rotational speed can affect the duration of the first stage is through the

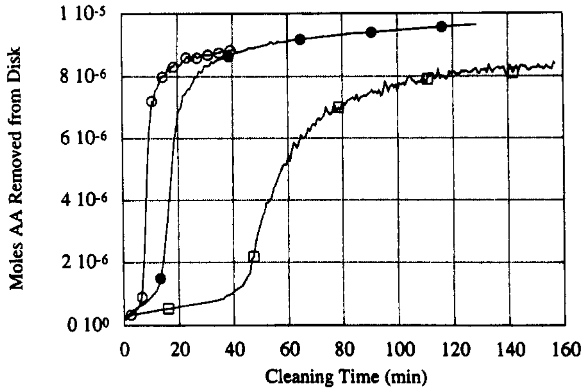

Figure 7. Effect of $C_{12}E_5$ concentration on cleaning: 1500 rpm, disks with 1 AA/IPA coat, 24 °C (○, 4.1×10^{-3} M $C_{12}E_5$; ●, 1×10^{-3} M $C_{12}E_5$; □, 6×10^{-5} M $C_{12}E_5$).

shear stress exerted on the film by the fluid flow over the disk. Increasing the shear rate at the disk surface will allow AA/IPA–$C_{12}E_5$ aggregates to be pulled from the film at lower extents of surfactant penetration and correspondingly higher film viscosities, both of which can result in first stages of shorter duration. It is probable that both of these effects contribute to the reduced duration of the first stage at higher disk rotational speeds.

The rate of AA removal in the second stage (slope of the cleaning curve) increases with increasing rotational speed of the disk. As discussed above, the shear stress at the disk surface is proportional to $\omega^{3/2}$, so that increasing the rotational speed of the disk increases the shear. This indicates that shear stresses at the disk surface may cause aggregates of the liquefied film to be pulled from the film and that higher shear rates allow aggregates to be removed more rapidly. Thus, a shear-controlled mechanism appears to be consistent with the observed behavior in the second stage. Another effect of the shear stress on the second stage is that at higher shear stress levels, the fraction of film removed during the second stage increases.

The rate of cleaning in the third stage also increases with the disk rotational speed, although the reduced cleaning rate in this stage compared to the second stage makes this effect less pronounced. This is consistent with the hypothesis that residual aggregates left over from the second stage are bound tightly to the FR-4 laminate, and it is these aggregates that are removed during the third stage.

Effect of $C_{12}E_5$ Concentration on Cleaning. The effect of the $C_{12}E_5$ concentration in solution on the three stages of cleaning is illustrated in Figure 7. The data in this figure are for disks with one AA/IPA coating, and the rotational speed was 1500 rpm. The results with three different surfactant concentrations are represented, 4.1×10^{-3}, 1×10^{-3} , and 6×10^{-5} M $C_{12}E_5$. The 6×10^{-5} M experiments are just below the cmc (6.4×10^{-5} M); this condition was selected to study the cleaning by nonmicellar solutions. The 1×10^{-3} M case shows the effect of micelles on the cleaning (compared to the nonmicellar solution), while the 4.1×10^{-3} M case shows the effect of a higher concentration of micelles on the cleaning. As can be seen from Figure 7, the duration of the first stage increases with increasing surfactant concentration. The partitioning results discussed previously showed that at equilibrium the surfactant partitioning into the films depended on the concentration of free surfactant in solution (either the submicellar concentration or the cmc (6.4×10^{-5} M) for the 1×10^{-3} and 4.1×10^{-3} M cases). However, the cleaning experiments show that the duration of the first stage is not constant for these three cases. The higher surfactant concentrations may speed up the transition from the first to the second stage in two ways. Micelles may adsorb on the film surface, releasing surfactant monomers at the interface and thus increasing the rate of monomer transport into the film. In addition, the micelles can aid in the incorporation of the liquefied AA film into the aqueous solution by speeding up the break up of droplets or aggregates from the surface. Both of these processes can decrease the duration of the first stage.

Figure 7 also shows that the rate of the second stage cleaning process is increased by increased surfactant concentration in solution. If desorption of AA solubilized in micelles controlled the second stage (as found by Shaeiwitz et al. (1981)) or if adsorption of micelles onto the films controlled this stage (as found by Carroll (1981) and Carroll et al. (1982)), it would be expected that negligible cleaning would occur in the absence of micelles. In fact, the rate of the second stage cleaning step is comparable in the 6.0×10^{-5} M system (below the cmc) and the systems above the cmc (4.1×10^{-3} and 1×10^{-3} M). This suggests that the cleaning during the second stage occurs by the same mechanism in the presence and absence of micelles, although the presence of micelles enhances the process. Raterman et al. (1984) found that increasing surfactant concentrations above the cmc increased the rate of solubilization of partially soluble solutes in a nonflow system. This is consistent with what is seen in Figure 7. As discussed above, micelles in solution may increase the rate at which surfactant monomer partitions onto the AA film. Micelles may also increase the rate of solubilization of AA aggregates. This is consistent with the results seen in Figure 7 where the rate of aggregate removal (slope of the second stage) is highest when the highest concentration of micelles is present (4.1×10^{-3} M), is intermediate when the low concentration of micelles is present (1×10^{-3} M), and is lowest when micelles are absent (6×10^{-5} M).

It can also be seen in Figure 7 that the rate of AA removal in the third stage increases with increasing bulk surfactant concentration. It is believed that the surfactant helps to reduce the interfacial tension at the AA–solution–laminate contact line to allow aggregate removal from the FR-4 surface, in accordance with the roll-up mechanism. As discussed previously, the third stage is characterized by the shear-induced removal of residual AA "islands" surrounded by bare FR-4 surface. The higher surfactant concentrations apparently increase the rate of the desorption process, although the effect is not as strong as that seen in the second stage.

Effect of Film Thickness on Cleaning. Figure 8 illustrates the effect of the initial AA/IPA film thickness on the cleaning at a fixed disk rotational speed (1750 rpm). The duration of the first stage increases dramatically with increases in the amount of AA/IPA initially present. During the first stage, if surfactant must penetrate into the films until a threshold level has been reached before the transition to the second stage may occur, then the initial thickness of the film will affect the duration of the stage. This is consistent with the liquefaction mechanism suggested, with the liquefaction process observed during the contacting experiments (above), and the penetration results of other authors on different systems (Aronson et al., 1983; Cox, 1990; Cox

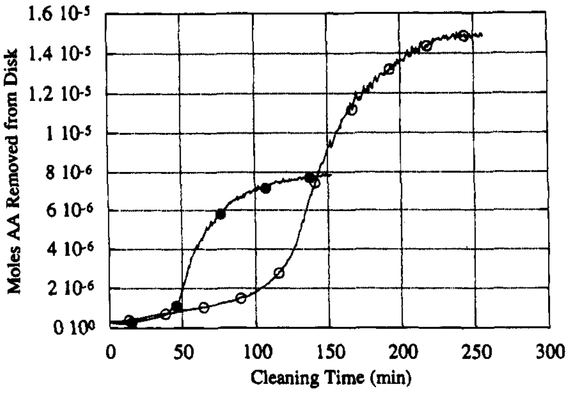

Figure 8. Effect of film thickness on cleaning: 6×10^{-5} M $C_{12}E_5$, 1750 rpm, 24 °C (○, disk with 3 AA/IPA coats; ●, disk with 1 AA/IPA coat).

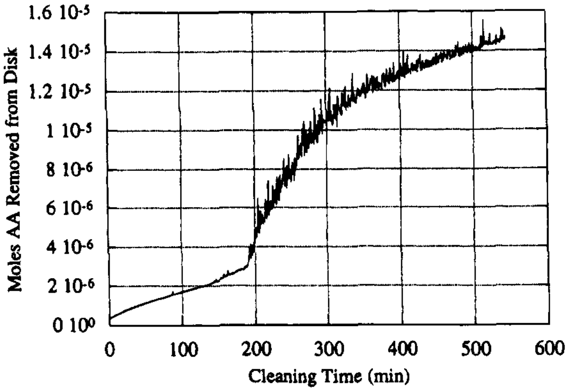

Figure 9. Aggregate removal during cleaning: 1×10^{-4} M $C_{12}E_5$, 700 rpm, disk with 2 AA/IPA coats, 24 °C.

et al., 1987; Dillan et al., 1979; Mankowich, 1961; McGuire and Matson, 1975; Schambil and Schwuger, 1987).

The rate of cleaning in the second stage (slope of cleaning curves) is essentially independent of the film thickness. This implies that once a certain concentration of surfactant has been attained in the film, the film viscosity will be low enough to allow the removal of film aggregates by shear forces at the disk surface, independent of how thick the film is initially. As the liquid film is being removed, surfactant will continue to penetrate the remaining organic film to maintain the low viscosity even in regions which had comparatively low surfactant contents at the start of the second stage (toward the FR-4–AA/IPA interface). Although the rate of film removal is independent of the initial film thickness, there is more film to be removed with the thick films than the thin films, so that the duration of the second stage increases with increasing film thickness.

The rate of the third stage cleaning is independent of the initial mass of the AA/IPA film. If the third stage cleaning occurs by shear-driven removal of aggregates ("islands") bound directly to the FR-4, it is expected that the third stage removal should be independent of the initial film mass. Rather, the mass of remaining material bound directly to the disk during the third stage should control the rate of removal during that stage.

Other Significant Cleaning Characteristics. Figure 9 presents the results of a cleaning experiment at a very low rotational speed (700 rpm) in which the aggregate nature of the cleaning during the second and third stages is particularly noticeable. The many small oscillations in the cleaning curve begin at the onset of the second stage and persist through the third stage. These oscillations are due to aggregates of AA/IPA–$C_{12}E_5$ which have been sheared from the surface and passed through the spectrophotometer before breaking down into smaller dispersed aggregates in solution. Comparison of Figure 9 with Figures 5–8 shows that the oscillations are less frequent and of smaller magnitude in experiments with higher disk rotational speeds. The higher the rotational speed of the disk, the greater the shear in the system and the greater the likelihood that aggregates will be broken up before entering the analytical loop. The cleaning solutions appeared clear at all times, so that the aggregates described are too small to be viewed with the naked eye or to cloud the solution.

Conclusions

The removal of mixed films of AA/IPA from FR-4 epoxy–glass laminate disks using aqueous solutions of $C_{12}E_5$ in a rotating disk apparatus was found to proceed in three stages. The important parameters that affect these stages are the thickness of the film initially present on the disk, the rotational speed of the disk, and the concentration of $C_{12}E_5$ in solution.

In the first cleaning stage, the surfactant penetrates into the AA/IPA film, resulting in liquefaction of the organic layer. The rate of penetration is increased by the rate of mass transfer of surfactant from the bulk solution to the disk surface, which is controlled by the disk rotational speed. The rotational speed also controls the shear rate at the disk surface. At higher shear-stress levels, the transition from the first (penetration) stage to the second (aggregate formation and removal) stage is facilitated. Higher overall surfactant concentrations facilitate the transition from the first to the second stage so that the duration of the first stage decreases with increasing surfactant concentration. Thick films result in longer durations for the first stage than thin films because surfactant must penetrate through a longer distance, and its concentration in the film must build up to a substantial level, before aggregate removal occurs (onset of second stage).

During the second stage, liquefied aggregates of AA/IPA film containing $C_{12}E_5$ are apparently sheared from the disk surface by the cleaning solution. The rate at which the aggregates are sheared from the surface is independent of the mass of film initially present on the disk, although the duration of the second stage is increased by increases in the initial film thickness. The presence of aggregates during the second and third stages is supported by the presence of spikes in the observed cleaning curves. Increases in the rotational speed of the disk increase the rate of aggregate removal by increasing the shear stress at the disk surface. Also, when the surfactant concentration in solution is increased, the rate of the second stage is increased, as the more concentrated solutions more rapidly lower the interfacial tension at the disk surface, enhancing the rate of aggregate formation and removal.

The third stage proceeds through the shear-driven removal of "islands" of AA directly bound to the FR-4 substrate. The rate of this stage is independent of the original mass of AA/IPA film on the disk, as it begins when most of the AA/IPA film has been sheared away. As in the second stage, when the shear stress or the surfactant concentration in solution is increased, the rate of the third stage increases.

In the companion paper to this work (part 2), theoretical models of the different cleaning stages have been developed and compared to the cleaning data presented above, with excellent agreement. These models consider the controlling processes in the first, second, and third stages to be penetration of the surfactant into the AA/IPA film, shear-driven removal of AA/IPA$-C_{12}E_5$ aggregates from the bulk AA film, and shear-driven removal of residual AA/IPA$-C_{12}E_5$ aggregates from the FR-4 laminate, respectively.

Acknowledgment

The authors would like to thank Northern Telecom Co. in Research Triangle Park, NC, for providing FR-4 laminate, and AT&T in Princeton, NJ, and the Digital Equipment Corp. in Augusta, ME, for their assistance in planning this work. Funding for this work was received from the Pollution Prevention Research Center at North Carolina State University and from the National Science Foundation Program for Environmentally Benign Chemical Synthesis and Processing (Grant No. CTS-9216850). The authors would also like to acknowledge Christine Palmer, Stacey Julien, and Rochelle Carlton for their assistance in the laboratory.

Nomenclature

D = diffusion coefficient for solute in solution, cm^2/s
k_m = mass transfer coefficient in fluid phase, cm/s
M_H = formula weight of hydrophilic portion of surfactant molecule, g
M_L = formula weight of hydrophobic portion of surfactant molecule, g
$Re = R^2\omega/\nu$ = Reynolds number in rotating disk, dimensionless
r = radial position on disk surface, cm
R = disk radius, cm

Greek Symbols

μ = viscosity of fluid, g/cm·s
ν = kinematic viscosity of fluid, cm^2/s
τ_{rz} = shear stress in axial direction on disk surface, $g/cm{\cdot}s^2$
ω = disk rotational speed, rad/s

Literature Cited

Albery, W. J.; Hitchman, M. L. *Ring Disc Electrodes*; Clarendon Press: Oxford, 1971.

Andersen, S. O. *Technical Progress on Protecting the Ozone Layer; Electronics, Degreasing, and Dry Cleaning Solvents Technical Options Report*; United Nations Environment Programme, 1989.

Aronson, M. P.; Gum, M. L.; Goddard, E. D. Behavior of Surfactant Mixtures in Model Oily-Soil Detergency Studies. *J. Am. Oil Chem. Soc.* **1983**, *60* (7), 1333.

Carroll, B. J. The Kinetics of Solubilization of Nonpolar Oils by Nonionic Surfactant Solutions. *J. Colloid Interface Sci.* **1981**, *79* (1), 126.

Carroll, B. J.; O'Rourke, G. C.; Ward, J. I. The Kinetics of Solubilization of Single Component Non-Polar Oils by a Non-Ionic Surfactant. *J. Pharm. Pharmacol.* **1982**, *34*, 287.

Chan, A. F.; Evans, D. F.; Cussler, E. L. Explaining Solubilization Kinetics. *AIChE J.* **1976**, *22* (6), 1006.

Chiu, Y. C.; Chen, L. J.; Pien, W. I. Mechanism Leading to Super-Detergent Power for Nonionic Surfactants. *Colloids Surf.* **1988**, *34*, 23.

Cobo, O. A.; Marchiano, S. L.; Arvia, A. J. Ionic Mass-Transfer at Rotating Electrodes Formed by Solids of Revolution. Rotating One-Base Spherical Segment Electrodes. *Electrochim. Acta* **1972**, *17*, 503.

Cochran, W. G. The Flow Due To A Rotating Disk. *Proc. Cambridge Philos. Soc.* **1934**, *30*, 365.

Cox, M. F. Surfactants for Hard-Surface Cleaning: Mechanisms of Solid Soil Removal. *J. Am. Oil Chem. Soc.* **1990**, *63* (4), 559.

Cox, M. F.; Smith, D. L.; Russell, G. L. Surface Chemical Processes for Removal of Solid Sebum Soil. *J. Am. Oil Chem. Soc.* **1987**, *64* (2), 273.

Daguenet, M. Study of Mass Transport in Solution Using Rotating Disk and Ring Electrodes. *Int. J. Heat Mass Transfer* **1968**, *11*, 1581.

Denison, J. W., Jr. Cleaning of Printed Circuit Boards to Remove Ionic Soils. *Mater. Perform.* **1975**, *14* (3), 36.

Dillan, K. W. Factors Affecting Oil/Water Interfacial Tension in Detergent Systems: Nonionic Surfactants and Nonpolar Oils. *J. Am. Oil Chem. Soc.* **1979**, *61* (7), 1278.

Dillan, K. W.; Goddard, E. D.; McKenzie, D. A. Oily Soil Removal from a Polyester Substrate by Aqueous Nonionic Surfactant Systems. *J. Am. Oil Chem. Soc.* **1979**, *56*, 59.

Ellison, B. T.; Cornet, I. Mass Transfer To A Rotating Disk. *J. Electrochem. Soc.* **1971**, *118* (1), 68.

Fort, T. J.; Billica, H. R.; Grindstaff, T. H., Studies of Soiling and Detergency. *J. Am. Oil Chem. Soc.* **1968**, *45*, 354.

Harris, J. C.; Anderson, R. M.; Satanek, J. Removal of Fatty Soil from Glass by Surfactants and Surfactant-Builder Compositions. *J. Am. Oil Chem. Soc.* **1961**, *38*, 123.

Langan, J. P. Reliability of Assemblies with Leave-On Flux. *3rd International SAMPE Electronics Conference*, 1989, p 813.

Levich, B. The Theory of Concentration Polarization. *Acta Physicochim. URSS* **1942**, *XVII* (5–6), 257.

Manko, H. H. *Soldering Handbook for Printed Circuits and Surface Mounting; Design Materials, Processes, Equipment, Trouble-Shooting, Quality, Economy, and Line Management*; Van Nostrand Reinhold: New York, 1986.

Mankowich, A. M. Hard Surface Detergency. *J. Am. Oil Chem. Soc.* **1961**, *38*, 589.

McGuire, S. E.; Matson, T. P. Nonbuilt Heavy Duty Liquids: Detergency and Formulating Parameters. *J. Am. Oil Chem. Soc.* **1975**, *52*, 411.

Middleman, S. The Effect of Induced Air-Flow on the Spin Coating of Viscous Liquids. *J. Appl. Phys.* **1987**, *62* (6), 2530.

Miller, C. A.; Raney, K. H. Solubilization-Emulsification Mechanisms of Detergency. *Colloids Surf. A.* **1993**, *74*, 169.

Mohr, C. M.; Newman, J. Mass Transfer to a Rotating Disk in Transition Flow. *J. Electrochem. Soc.* **1976**, *123* (11), 1687.

Mori, F.; Lim, J. C.; Raney, O. G.; Elsik, C. M.; Miller, C. A. Phase Behavior, Dynamic Contacting, and Detergency in Systems Containing Triolein and Nonionic Surfactants. *Colloids Surf.* **1989**, *40*, 323.

Nakagawa, T.; Nakagawa, T. K. Solubilization of Long Chain Alkyl Compounds by a Non-Ionic Surfactant, and Clouding Formation Observed in Such Systems. *Kolloid Z.* **1960**, *168*, 132.

Neogi, P.; Kim, M.; Friberg, S. E. Hydrocarbon Extraction Into Surfactant Phase with Nonionic Surfactants. II. Model. *Sep. Sci. Technol.* **1985**, *20* (7 & 8), 613.

Newman, J. Schmidt Number Correction for the Rotating Disc. *J. Phys. Chem.* **1966**, *70* (4), 1327.

Newman, J. *Electrochemical Systems*; Prentice Hall: Englewood Cliffs, NJ, 1973.

Raney, K. H.; Miller, C. A. Optimum Detergency Conditions with Nonionic Surfactants: II. Effect of Hydrophobic Additives. *J. Colloid Interface Sci.* **1987**, *119* (2), 539.

Raney, K. H.; Benson, H. L. The Effect of Polar Soil Components on the Phase Inversion Temperature and Optimum Detergency Conditions. *J. Am. Oil Chem. Soc.* **1990**, *67* (11), 722..

Raney, K. H.; Benton, W. J.; Miller, C. A. Optimum Detergency Conditions with Nonionic Surfactants. I. Ternary Water-Surfactant-Hydrocarbon Systems. *J. Colloid Interface Sci.* **1987**, *117* (1), 282.

Raterman, K. T.; Adams, K. L.; Shaeiwitz, J. A. Liquid Solubilization Dynamics. *J. Colloid Interface Sci.* **1984**, *98* (2), 406.

Riza, F. A.; Kesavan, S. Substitutes and Alternatives to CFC-113 Based Cleaning - An Overview. *The 3rd International SAMPE Electronics Conference*, 1989, p 804.

Rosen, M. J. *Surfactants and Interfacial Phenomena*; John Wiley and Sons: New York, 1989.

Sayeed, F. A. A.; Schott, H. Micellar Solubilization of Cholesteryl Esters of C_{18} Fatty Acids by a Nonionic Surfactant. *J. Colloid Interface Sci.* **1986**, *109* (1), 140.

Schambil, F.; Schwuger, M. J. Correlation Between the Phase Behavior of Ternary Systems and Removal of Oil in the Washing Process. *Colloid Polym. Sci.* **1987**, *265* (11), 1009.

Schlicting, H. *Boundary Layer Theory*, 6th ed.; McGraw-Hill: New York, 1968.

Schott, H. Hydrophile-Lipophile Balance and Cloud Points of Nonionic Surfactants. *J. Pharm. Sci.* **1969**, *58* (12), 1443.

Schott, H.; Sayeed, F. A. A. Micellar Solubilization of Cholesterol and of Mixtures of Cholesterol with Cholesteryl Esters of C_{18} Fatty Acids by a Nonionic Surfactant. *J. Colloid Interface Sci.* **1986**, *112* (1), 144.

Shaeiwitz, J. A.; Chan, A. F.-C.; Cussler, E. L.; Evans, D. F. The Mechanism of Solubilization in Detergent Solutions. *J. Colloid Interface Sci.* **1981**, *84* (1), 47.

Strong, L.; Middleman, S. Lubricant Retention on a Spinning Disk. *AIChE J.* **1989**, *35* (10), 1753.

Tokiwa, F. Solubilization Behavior of Sodium Dodecylpolyoxyethylene Sulfates in Relation to Their Polyoxyethylene Chain Lengths. *J. Phys. Chem.* **1968**, *72* (4), 1214.

Van Hunsel, J.; Bleys, G.; Joos, P. Adsorption Kinetics at the Oil/Water Interface. *Colloid Polym. Sci.* **1986**, *114* (2), 432.

Wang, D. W. Advanced Materials for Printed Circuit Boards. *Mat. Res. Soc. Symp: Electron. Packag. Mater. Sci. III* **1988**, *108*, 125.

White, R.; Mohr, C. M.; Newman, J. The Fluid Motion Due To a Rotating Disk. *J. Electrochem. Soc.* **1976**, *123* (3), 383.

Woodgate, R. W. *Handbook of Machine Soldering, A Guide for the Soldering of Electronic Printed Wiring Assemblies*; John Wiley and Sons: New York, 1983.

Received for review January 3, 1995
Revised manuscript received May 23, 1995
Accepted June 14, 1995[⊗]

IE950014R

[⊗] Abstract published in *Advance ACS Abstracts,* August 15, 1995.